

Investigation on the competing effects of clay dispersion and matrix plasticisation for polypropylene/clay nanocomposites. Part II: Crystalline structure and thermo-mechanical behaviour

Yu Dong ^{a,*}, Debes Bhattacharyya ^b

^a *Department of Mechanical Engineering, Curtin University of Technology
GPO Box U1987, Perth, WA 6845, Australia*

^b *Centre for Advanced Composite Materials, Department of Mechanical Engineering
The University of Auckland, Private Bag 92019
Auckland, New Zealand*

Abstract

In view of the structure-property relationship, the mechanical property enhancement of polypropylene (PP)/clay nanocomposites can also be associated with the alterations of their crystalline structures and crystalline behaviour in addition to the general interpretation of intercalation/exfoliation level and uniform dispersion of more rigid clay platelets at higher aspect ratios in the PP matrix. Wide angle X-ray diffraction (WAXD) was utilised to evaluate the effects of clay content, maleated PP (MAPP) content (MAPP as the compatibiliser) on PP crystalline structures of nanocomposites. Furthermore, the melting and crystallisation behaviour of PP/clay nanocomposites was also investigated by conducting differential scanning calorimetry (DSC). The thermo-mechanical properties were characterised via dynamic mechanical thermal analysis (DMTA). It is observed that enhancement of mechanical properties are mainly affected by the preferred orientation of PP crystals, the growth of α -PP phase and effective nucleating agent role of additional clay while the excessive amount of MAPP becomes detrimental to these crucial aspects, which is also evidently revealed in DMTA measurements.

* Corresponding author. Tel.: +61 8 92669055; fax: +61 8 92662681.
E-mail address: Y.Dong@curtin.edu.au (Y. Dong).

Keywords: Nanocomposites; Nanoclays; Mechanical properties; Thermal analysis; Crystallisation structure

1. Introduction

At the advent of fabricating polymer/clay nanocomposites as one of the most innovative materials, the considerable attention has been gained in that homogeneous dispersion of clay platelets with high aspect ratios into continuous polymer matrix at low filler contents leads to the dramatic property enhancements such as increased stiffness and strength [1-4], better barrier properties [5, 6] and more favourable dimensional stability [7]. The clay dispersability [8-10] and the increase of the interfacial areas with active interactions [11, 12] between clay platelets and the PP matrix are often considered as the main contributors to influence the efficiency of the property enhancement.

However, the polymer matrices like nylon 6, polypropylene (PP) and polyethylene (PE) used in the melt compounding of nanocomposites contain the crystalline structures which also enable to significantly affect the physical and mechanical properties of nanocomposites with the additional clay. Early work by Liu et al. [1] on melt intercalation of nylon 6/clay nanocomposites suggests that the addition of clay has the effect of promoting the formation of the γ -crystalline form, increases the crystallisation temperature of nylon 6 and narrows the width of crystalline peak. Further study by Fornes and Paul [13] indicates the “skin-core” effect of nylon 6 nanocomposites with the sample skin layer containing only γ -crystalline form while with the core region having both α and γ forms. More interestingly, the presence of clay enhances the γ form with higher level of crystallinity in the skin but has little effect on crystalline structure in the core. In the other aspect, Nam et al [14] again confirms the existence of γ form with the addition of clay due to the narrow space

surrounded by the dispersed clay and the intercalation of the PP chains. In contrast, Perrin-Sarazin et al. [15] claims that the better clay dispersion in the presence of MAPP leads to a crystallisation at lower temperature and lower rate but does not affect the level of crystallinity. Moreover, by investigating PP and nylon 6 alloys/clay nanocomposites, Tang et al. [16] demonstrates that the blend sequences have influence on crystalline structure and a higher cooling rate results in increasing of γ form. Consequently, it is essential to understand the possible factors to influence the formation or enhancement of the crystalline forms and the related mechanical properties.

As a supplementary part of discussion for the preceding paper [17], the aim of this work is to examine the effects of clay and MAPP contents on the crystalline structures and behaviour of PP/clay nanocomposites formed by melt compounding process in relation to their enhanced mechanical properties.

2. Experimental Details

2.1 Materials and nanocomposite preparation

PP/clay nanocomposites were prepared by melt compounding the mixtures of PP homopolymer H380F (density: 0.9 g/cm^3 , melt flow index MFI = 25 g/10 min at 230°C and 2.16 kg), MAPP Exxelor™ PO1020 (MA content: 0.5-1 wt%, MFI= ~430 g/10min at 230°C and 2.16 kg) and NANOLIN™ DK4 organoclay (density: 1.8 g/cm^3 and interlayer spacing: $d_{001} = 3.56 \text{ nm}$). Three typical material formulations used in this study are listed in Table 1. The nanocomposite pellets were dried and then injection moulded into standard mechanical testing samples and strip-like samples. The further details for the melt processing procedure have been elaborated in the previous papers [17, 18].

2.2 Characterisation and measurements

2.2.1 Wide angle X-ray diffraction (WAXD)

Wide angle X-ray diffraction (WAXD) is a sophisticated characterisation technique for the evaluation of any consistent and ordered material structures. In particular, for the semi-crystalline polymers such as polypropylene (PP) and polyethylene (PE), the crystalline structures can also be investigated via WAXD in order to understand how the transformation of crystal phase alters the physical and mechanical properties of their nanocomposites due to the addition of clay. A Bruker D8 ADVANCE diffractometer was used at 40 kV and 40 mA with Cu- k_{α} X-ray beam (wave length $\lambda=0.154$ nm) to conduct the WAXD analysis at room temperature. The WAXD patterns were obtained in a wide angle range of $2\theta=2-30^{\circ}$ at a scan rate of $0.4^{\circ}/\text{min}$.

2.2.2 Differential scanning calorimetry (DSC)

DSC is a thermal analytical technique where the difference in the amount of heat required to increase the temperature of a sample and reference are measured as a function of temperature. A DSC-Q1000 TA instrument was employed to study the melting and crystallisation behaviour of PP/clay nanocomposites under the nitrogen atmosphere. Prepared DSC sample around 10 mg was cut from an injection moulded strip-like sample and sealed in an aluminium pan using a sample encapsulation press. Then it was further placed into the DSC cell by an automatic sample gripper with the reference to the sealed empty pan. The DSC sample was first equilibrated at -60°C , heated up to 220°C at the heating rate of $10^{\circ}\text{C}/\text{min}$, and subsequently underwent the isothermal condition for 5 mins to eliminate any thermal history of tested materials. Then, it was cooled down to -60°C at the cooling rate of $10^{\circ}\text{C}/\text{min}$. The identical

procedure was carried out for a second run. The final crystallisation and melting curves were selected from the first cooling and second heating scans, respectively.

The melting temperature (T_m), crystallisation temperature (T_c) and degree of crystallinity (X_c) of the PP matrix in PP/clay nanocomposites were determined from the DSC measurement. X_c was evaluated from the following relationship:

$$X_c (\%) = \frac{\Delta H_m}{(1 - W_f) \Delta H_f^0} \times 100 \quad (1)$$

where ΔH_m (J/g) is the heat of fusion of PP matrix, W_f is the weight fraction of clay particles and ΔH_f^0 is the heat of fusion of pure crystalline PP ($\Delta H_f^0 = 209$ J/g [19]).

2.2.2 Dynamic mechanical thermal analysis (DMTA)

DMTA is a material characterisation tool to determine the viscoelastic properties by evaluating the dynamic elastic modulus E' , loss modulus E'' and loss tangent $\tan\delta$ ($\tan\delta = E''/E'$) under applied stress, frequency and temperature. A Rheometric Scientific DMTA V analyser was utilised in a single cantilever mode at 0.01% strain with an oscillatory frequency of 1Hz. The DMTA temperature ranged from -60 to 150°C at a heating rate of 5°C/min in the nitrogen atmosphere. The DMTA samples with the nominal dimensions of 27×10×2.5 mm were cut from the injection moulded strip-like samples. At least two samples were used at each measurement for the test reproducibility. The glass transition temperature (T_g) was determined based on the peak of $\tan\delta$ as a sensitive indicator of transitions in this study.

3. Results and Discussion

3.1.1 Crystalline structures

The crystalline structures of neat PP, MAPP and corresponding PP/clay nanocomposites in three typical formulations were investigated with WAXD patterns depicted in Figs. 1-3. For formulation type I and II, it is observed that five

characteristic peaks of most common α -PP structure appear in all the materials at 2θ angles of about 14.0, 16.8, 18.6, 21.2 and 21.9°, corresponding to lattice planes of (110), (040), (130), (111) and (131), respectively [20, 21], Figs. 1 and 2. Despite the different relative peak intensities, the detection of the same number of WAXD peaks as those of neat PP implies that the addition of clay does not greatly affect the crystalline structures of PP matrix in such nanocomposites.

Since induced crystalline structure can be revealed in the PP matrix when injection moulded with the mineral fillers such as talc, mica, clay, etc., its crystal orientation can be very critical to influence the nucleation, crystallisation, morphology and resulting mechanical properties [22]. In order to evaluate the relative degree of PP orientation, the ratio of peak intensity areas of (110) and (040), denoted as $I_{(110)}/I_{(040)}$, were measured from obtained WAXD patterns relative to the clay content in material formulation types I and II, and to the MAPP content in type III, respectively, Figs. 4 and 5. The isotropic PP region was determined by Rybníkář [23] in the range of 1.3-1.5. Accordingly, the larger deviation was found from this range, the more preferred PP orientation occurs. The $I_{(110)}/I_{(040)}$ ratio of neat PP used in this study is approximately 1.66, which signifies its nearly isotropic material nature with homogeneity; whereas low molecular weight MAPP possesses a relatively high crystal orientation with the peak intensity ratio of 2.03. The peak intensity ratios (0.06-0.24) for both formulation type I and type II are far below those of isotropic PP region. In addition, the orientation level of PP crystals improves remarkably for Type II but shows the retention trend for type I with increasing the clay content. This finding might result in the better enhanced mechanical properties determined in type II in our previous work [17] since the embedded clay particles as effective nucleators could accelerate the PP crystallisation process with higher crystal orientation (seen in

type II) that often provides the higher flexural modulus, flexural strength and mould shrinkage for nucleator-added PP composites in the structure-property relationship [24]. When the effect of MAPP content on the peak intensity ratio was investigated, it has been found that with increasing MAPP content, $I_{(110)}/I_{(040)}$ ratio initially declines sharply from 0.44 (0 wt% MAPP) to 0.10 (3 wt% MAPP) and then increases monotonically up to 0.31 at the maximum MAPP content of 20 wt%. The lowest ratio at 3 wt% MAPP indicates the largest deviation from the isotropic PP region, thus reflecting the highest preferred orientation of PP crystals which coincides with the maximum enhancements of tensile and flexural properties taking place within the MAPP saturation level of 3-6 wt% determined in our previous study [17].

From the other point of view, an overall significant alteration in the intensity of α (040) becomes quite manifested and all the nanocomposites reveal more considerably enhanced α (040) peak intensities compared to those of neat PP and MAPP, Figs. 1-3. As mentioned in the literatures [25, 26], the formation of α -PP mainly contributes to the improvement of tensile modulus and better yield stress, also in good accordance with previously determined tensile properties for formulation types I and II [17]. In particular, the α (040) intensity is relatively reduced for formulation type I with increasing the clay content, as compared to the insignificant intensity change for type II as depicted in Figs. 1 and 2. This difference might be ascribed to the addition of low molecular weight MAPP that lowers the α (040) intensity, which has expectedly little effect on the transformation of crystalline structures. With respect to type III, PP/clay nanocomposites without MAPP (i.e. MAPP0) appear to contain both α -PP and β -PP formations. Since β -PP can induce better impact resistance and greater elongation at break relative to α -PP [25, 26], the existence of β -PP, to a certain extent, could lead to the predetermined higher impact strength measured for MAPP0 in spite

of large clay tactoids observed in its morphological structure [17]. Nevertheless, β -PP formation tends to disappear in the WAXD peaks in the presence of MAPP. Similarly, increasing the MAPP content from 3 to 20 wt% results in the dramatic reduction of α (040) peak intensity. In view of the crystalline phases, it is very evident that at a fixed clay content, increasing the MAPP content enables to prevent the further growth of α -PP, thus leading to the lower tensile properties of such nanocomposites at a higher MAPP content [17]. As a result, the mechanical properties of PP/clay nanocomposites can be influenced by both α -PP and β -PP crystalline structures of the PP matrix despite the predominant constituent of more stable α -PP form, often existing in the melt-crystallisation process.

3.1.2 Melting and crystallisation behaviour

The influences of clay and MAPP contents on the melting and crystallisation behaviour of PP/clay nanocomposites were characterised by DSC thermal analysis, Figs. 6-8. The corresponding characteristic parameters and calculated level of crystallinity (X_c) are also presented in Table 2. All nanocomposites possess melting temperatures (T_m) at approximately 164°C regardless of the clay and MAPP contents, which is quite similar to those of neat PP and MAPP. This phenomenon suggests that the coexistence of clay and MAPP has little effect on the melting behaviour of PP/clay nanocomposites relative to neat PP.

With respect to the crystallisation behaviour, the crystallisation temperatures (T_c) of nanocomposites in formulation type I unanimously increase up to 118°C irrespective of the clay content, as compared to 113°C for neat PP and 112°C for MAPP accordingly. Such increase might be ascribed to a good balance between positive nucleating effect of clay and the detrimental influence of the excessive amount of MAPP which perhaps goes into the PP bulk matrix and tends to inhibit and

further randomise the nucleation to some extent. Moreover, a better clay dispersion along with more active interfacial interactions could induce more nucleating cores to facilitate the crystallisation process with the better nucleating effect and the higher T_c [27]. The higher T_c of such nanocomposites is also indicative of a higher extent of segregation of dispersed clay platelets possibly around the boundary of the spherulites/interspherulites, resulting in the enhanced intercalation [17, 28]. The X_c of nanocomposites in type I slightly increases up to 46.3% compared to 41.8% for neat PP, again implying the positive nucleating effect of dispersed clays on crystallinity. Even though MAPP is deemed as high crystalline PP with the X_c value of 92.3%, it has minimal influence on the crystallinity degree of all nanocomposite counterparts.

As for formulation type II, the T_c is considerably enhanced with increasing the clay content and reaches the maximum temperature of 120°C for PPNC10. This finding is partly due to the predominant role of clay as a nucleating agent as opposed to the less severe matrix plasticisation effect caused by the used moderate amount of MAPP. By contrast, the X_c for formulation type II becomes higher than that of type I with the maximum level up to over 48% for PPNC5 and PPNC10. The additions of MAPP and clay appear to make the totally opposite contributions to the crystallisation behaviour of PP/clay nanocomposites. The T_c values could be lowered owing to the anti-nucleating effect of MAPP when increasing its content; whereas when the good clay dispersion along with the active interfacial interactions are achieved, the growth of nucleating cores and reduction of spherulite size become dominant with embedded clays.

As for formulation type III, when no compatibiliser is used in MAPP0, the addition of clay substantially increases the T_c up to 121°C owing to the conventional heterogeneous nucleation effect though no favourable interfacial interactions exist.

Nonetheless, with increasing the MAPP content, the T_c is relatively reduced to 117°C for MAPP20 (20 wt% MAPP), but is still present well above that of neat PP. This observation validates the aforementioned hypothesis that a compromising result has to be made to reflect the crystallisation behaviour due to the counteractive nucleating roles of clay and MAPP. Moreover, the X_c seems not to be significantly influenced, and still remain at a relatively high level compared to that of neat PP.

Hence, the nucleating effect of clay is very crucial to enhance the mechanical and thermal properties since the surface-nucleated crystalline phase has better mechanical and thermal characteristics than the neat polymer crystal phase [27]. The crystallisation behaviour presented in this study is in good accordance with the enhanced mechanical properties of nanocomposites from the previous paper [17]. Unfortunately, the glass transition temperature (T_g) shows a very weak appearance in DSC analysis, but it can be better detected by performing more sensitive DMTA measurements.

3.7 Dynamic mechanical properties

The reinforcement effect, due to the additional clay and MAPP, and the glass transition temperature (T_g) are of great concern in this study. The dynamic elastic modulus E' and loss tangent $\tan\delta$ as a temperature function for PP/clay nanocomposites are exhibited in Figs. 9-11. The representative values of E' at five specific temperatures ranging from -30 to 135°C as well as the T_g values are listed in Table 3. During the experimental tests, two relaxations are observed in neat PP and nanocomposites, clearly identified as α and β peaks. α peak of PP crystalline regions is considered as the shoulder-like weak peak close to 100°C while β peak represents the glass-rubber relaxation of the PP amorphous portion, normally assigned to T_g [19].

As evidenced in Figs. 9 and 10, most nanocomposites in formulation types I and II demonstrate much higher T_g compared to neat PP ($T_g = 14.7^\circ\text{C}$). A further enhanced T_g up to the maximum value of 21°C is revealed by increasing the clay content from 5 to 10 wt%. This phenomenon could mainly benefit from the uniform clay dispersion and the active interfacial interactions between PP molecular chains and intercalated clay platelets. Besides, the more intercalated clay platelets are shown, the higher restriction of PP chains mobility can be anticipated, leading to the shift of T_g to a higher temperature. On the other hand, below the T_g , a substantial increase of elastic modulus is recorded by over 40% with increasing the clay content in the presence of MAPP. All the nanocomposites have expectedly higher elastic moduli than neat PP. Even at higher temperatures above T_g , the elastic modulus continues to increase at a low clay content up to 5 wt% with the maximum improvement of 42% at 135°C for Opt1, PPNC3 and PPNC5. Conversely, the modulus enhancement becomes less pronounced around 17-30% at high clay contents (8-10 wt%). This finding indicates that the remarkable reinforcement effect can still take place in the rubbery plateau, depending on a good clay dispersion and favourable interfacial interactions, which are certainly achieved more easily at low clay contents.

Owing to its important role in diminishing the clay agglomeration, the effect of MAPP content on the thermo-mechanical behaviour of nanocomposites in formulation type III is also demonstrated in Fig. 11. The elastic moduli of nanocomposites are much higher than those of neat PP in the whole temperature range. However, it can be seen that all the nanocomposites present very close moduli versus temperature curves despite the greatest modulus improvement found in MAPP3 which reflects correspondingly the most preferred orientation of PP crystals in Fig.5. In particular, at room temperature, with increasing the MAPP content, a

similar threshold trend becomes manifested with the modulus enhancement up to 25% for MAPP3, in good agreement with obtained corresponding flexural properties of such nanocomposites [17] where the highest flexural modulus takes place at 3 wt% MAPP. Consequently, the use of 3 wt% MAPP can be suggested as the optimum level given that increased stiffness is the main design objective in type III. The declining tendency of elastic modulus at the high MAPP content again suggests that the excessive amount of low molecular weight MAPP softens nanocomposites due to its matrix plasticisation effect [17], which acts at the edge of clay platelets rather than penetrate into the clay interlayer areas. In the other aspect, increasing the MAPP content from 0 to 6 wt% is prone to less severe impact on the T_g of nanocomposites, which levels off or becomes slightly higher around 15°C. When the higher MAPP content (10-20 wt%) is incorporated, the T_g gradually increases from 18 to 22°C, signifying that the addition of MAPP as a compatibiliser can promote the clay dispersability, and thus make the mobility of PP chains less active. Therefore, a balance between the stiffness and the amount of compatibiliser is required to achieve the better mechanical property enhancement of PP/clay nanocomposites.

4. Conclusions

The crystalline structure and thermo-mechanical behaviour of PP/clay nanocomposites formed by melt processing were thoroughly investigated. In WAXD analysis, the presence of clay was found not to significantly alter the crystalline structures of nanocomposites with the same number of WAXD peaks as observed in neat PP. However, the peak intensities of α (040) in the α -PP formation and preferred orientation of PP crystals reflected from the $I_{(110)}/I_{(040)}$ ratio have been considerably enhanced, which is believed to contribute to the improvements of tensile and flexural properties of nanocomposites. In addition, it is quite evident that the excessive amount

of MAPP hinders the growth of α -PP, thus lowering the tensile properties of nanocomposites with a high MAPP content.

In DSC analysis, very little effect of the additional clay in the PP matrix is detected on the melting behaviour of nanocomposites while PP/clay nanocomposites show the overall higher crystallisation temperatures and slightly better enhancement levels of crystallinity compared to neat PP. It is confirmed that the addition of clay plays a significant role as the nucleating agent, leading to the greater mechanical property enhancement of nanocomposites. However, an excessive amount of MAPP becomes more or less anti-nucleators. A good balance needs to be achieved between the amounts of clay and MAPP to facilitate the crystallisation of PP/clay nanocomposites.

DMTA measurements reveal that the enormous reinforcement effect takes place in PP/clay nanocomposites with the modulus improvement of over 40% at a high clay content (8-10 wt%) and temperature below the T_g . Such enhancement tendency is conversely well maintained at a low clay content (≤ 5 wt%) in the rubbery plateau. It is also manifested that the excessive amount of MAPP as a soft plasticiser can also reduce the thermo-mechanical properties of PP/clay nanocomposites. The glass transition temperatures (T_g) of most nanocomposites also increase compared to that of neat PP, resulting from the intercalated structures to restrict the mobility of PP molecular chains.

Acknowledgements

This work was financially supported by Tertiary Education Commission (TEC), New Zealand to Dr. Yu Dong through the Bright Future Top Achiever Doctoral Scholarship during his PhD studies and also by Foundation for Research, Science and Technology (FRST), New Zealand under the FRST grant # UOAX 0406.

References

- [1] Liu L, Qi Z, Zhu X (1999) *J Appl Polym Sci* 71:1133-1138.
- [2] Kojima Y, Usuki A, Kawasumi M, Okada A, Fukushima Y, Kurauchi T, Kamigaito O (1993) *J Mater Res* 8: 1185-1189.
- [3] Hasegawa N, Kawasumi M, Kato M, Usuki A, Okada A (1998) *J Appl Polym Sci* 67: 87-92.
- [4] Liu XH, Wu QJ (2001) *Polymer* 42:10013-10019.
- [5] Messersmith PB, Giannelis EP (1995) *J Polym Sci Part A* 33:1047-1057.
- [6] Giannelis EP (1998) *Appl Organomet Chem* 12: 675-680.
- [7] Garcés JM, Moll DJ, Bicerano J, Fibiger R, Mcleod DG (2000) *Adv Mater* 12: 1835-1839.
- [8] Chavarria F, Paul DR (2004) *Polymer* 45: 8501-8515.
- [9] Lertwimolnun W, Vergnes B (2005) *Polymer* 46: 3462-3471.
- [10] Paul DR, Robeson LM (2008) *Polymer* 49: 3187-3204.
- [11] Oya A (2000) In: Pinnavaia TJ, Beall GW (ed) *Polymer-clay nanocomposites*, John Wiley & Sons, New York, p. 151-172.
- [12] Alexandre M, Dubois P (2000) *Mater Sci Eng* 28: 1-63.
- [13] Fornes TD, Paul DR (2003) *Polymer* 44: 3945-3961.
- [14] Nam PH, Maiti P, Okamoto M, Kotaka T, Hasegawa N, Usuki A (2001) *Polymer* 42: 9633-9640.
- [15] Perrin-Sarazin F, Ton-That MT, Bureau MN, Denault J (2005) *Polymer* 46: 11624-11634.
- [16] Tang Y, Hu Y, Zhang R, Gui Z, Wang Z, Chen Z, Fan W (2004) *Polymer* 45: 5317-5326.
- [17] Dong Y, Bhattacharyya D. Investigation on the competing effects of clay dispersion and matrix plasticisation for polypropylene/clay nanocomposites. Part I: Morphology and mechanical properties. Submitted to *J Mater Sci*.
- [18] Dong Y, Bhattacharyya D (2008) *Compos Part A* 39: 1177-1191.
- [19] Mark JE (1996) *Physical properties of polymer handbook*, AIP Press, New York.
- [20] Zhao L, Li J, Guo S, Du Q (2006) *Polymer* 47: 2460-2469.
- [21] Zheng Q, Shangguan Y, Yan S, Song Y, Peng M, Zhang Q (2005) *Polymer* 46: 3163-3174.
- [22] Alonso M, Velasco JI, de Saja JA (1997) *Eur Polym J* 33: 255-262.

- [23] Rybníkář F (1989) J Appl Polym Sci 38:1479-1490.
- [24] Fujiyama M, Wakino T (1991) J Appl Polym Sci 42 : 2739-2747.
- [25] Tjong SC, Shen JS, Li RKY (1996) Polym Eng Sci 36: 100-105.
- [26] Karger-Kocsis J, Varga J (1996) J Appl Polym Sci 62: 291-300.
- [27] Lei SG (2003) Formulation and mechanical properties of polypropylene nanocomposites. M.ASc thesis, Department of Mechanical and Industrial Engineering, Concordia University, Montreal, Canada.
- [28] Maiti P, Nam PH, Okamoto M, Hasegawa N, Usuki A (2002) Macromolecules 35: 2042-2049.

List of Figures

Fig. 1 WAXD patterns of neat PP, MAPP and PP/clay nanocomposites in formulation type I. The curves are shifted vertically for clarity.

Fig. 2 WAXD patterns of neat PP, MAPP and PP/clay nanocomposites in formulation type II. The curves are shifted vertically for clarity.

Fig. 3 WAXD patterns of neat PP, MAPP and PP/clay nanocomposites in formulation type III. The curves are shifted vertically for clarity.

Fig.4 Dependence of peak intensity ratio $I_{(110)}/I_{(040)}$ on clay content for formulation types I and II.

Fig.5 Dependence of peak intensity ratio $I_{(110)}/I_{(040)}$ on MAPP content for formulation type III.

Fig. 6 DSC curves of neat PP, MAPP and PP/clay nanocomposites in formulation type I: (a) heating scan and (b) cooling scan. The curves are shifted vertically for clarity.

Fig. 7 DSC curves of neat PP, MAPP and PP/clay nanocomposites in formulation type II: (a) heating scan and (b) cooling scan. The curves are shifted vertically for clarity.

Fig. 8 DSC curves of neat PP, MAPP and PP/clay nanocomposites in formulation type III: (a) heating scan and (b) cooling scan. The curves are shifted vertically for clarity.

Fig. 9 DMTA curves for neat PP and PP/clay nanocomposites in formulation type I: (a) dynamic elastic modulus E' and (b) loss tangent $\tan\delta$.

Fig. 10 DMTA curves for neat PP and PP/clay nanocomposites in formulation type II: (a) dynamic elastic modulus E' and (b) loss tangent $\tan\delta$.

Fig. 11 DMTA curves for neat PP and PP/clay nanocomposites in formulation type III: (a) dynamic elastic modulus E' and (b) loss tangent $\tan\delta$.

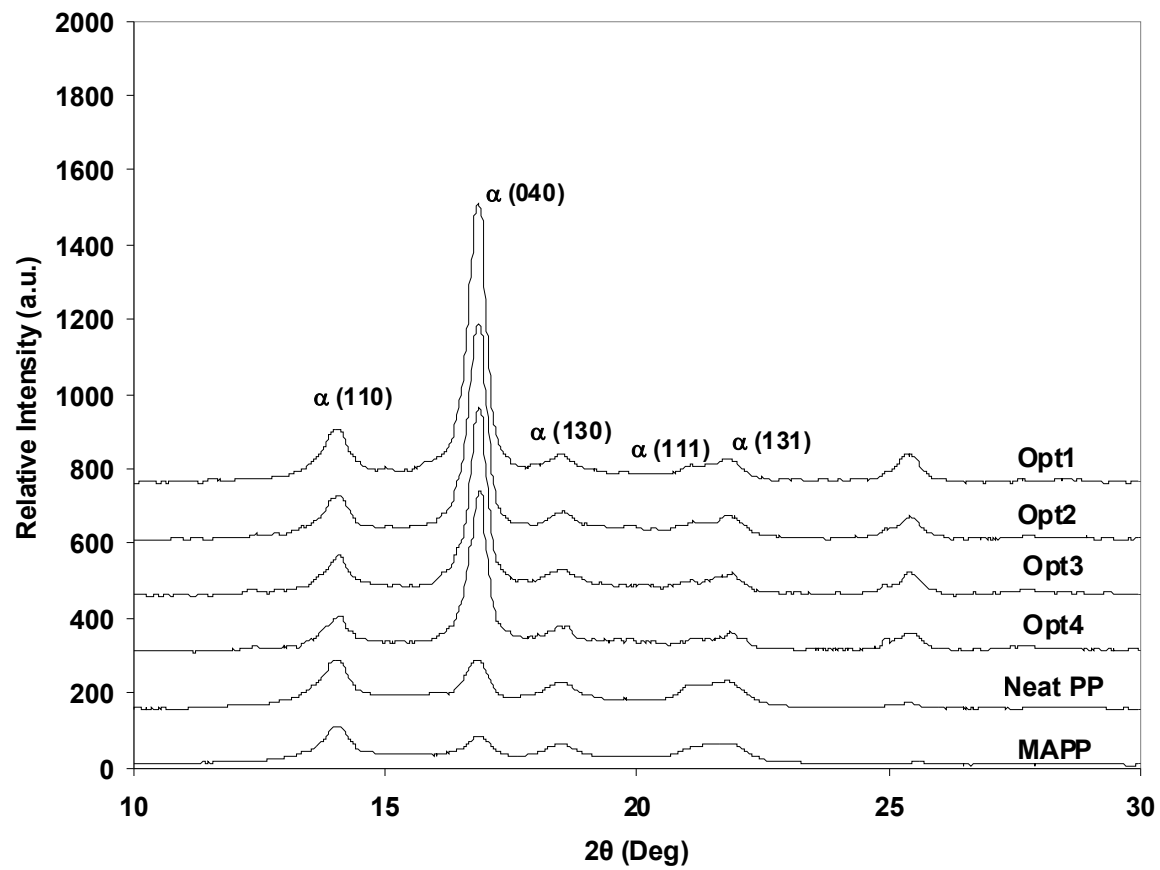


Fig. 1

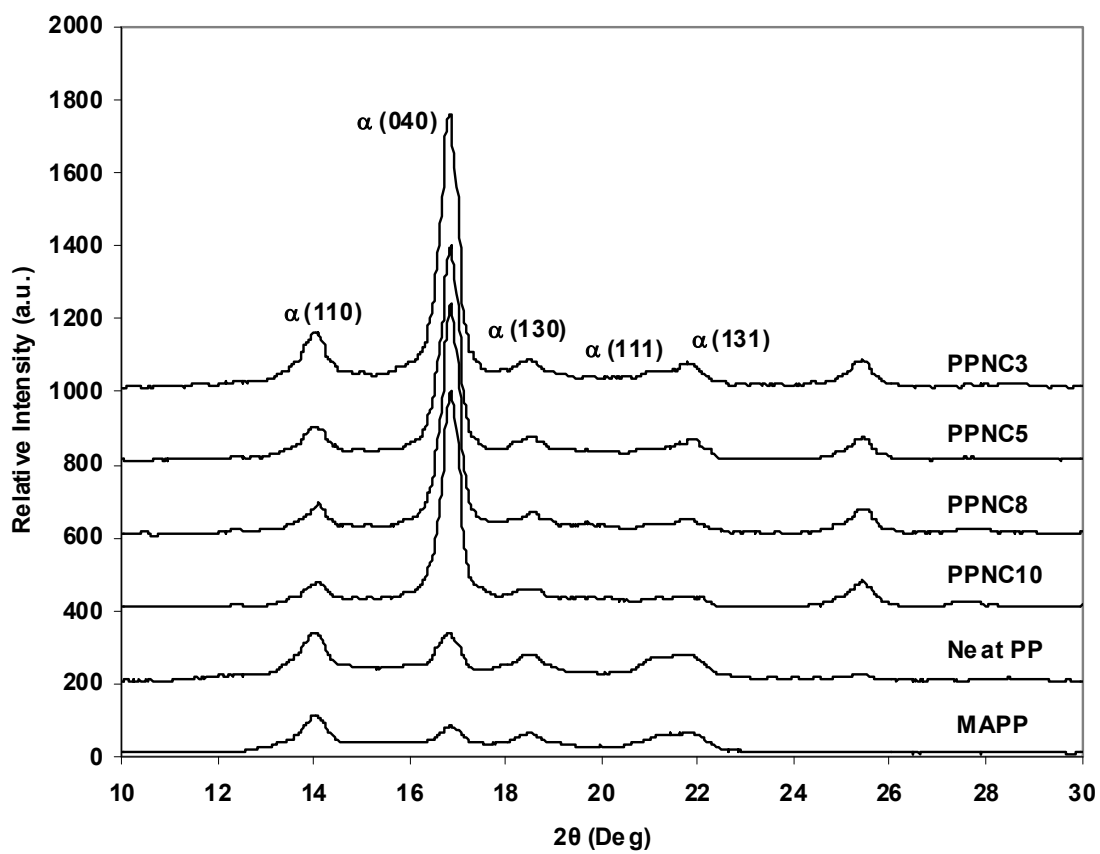


Fig. 2

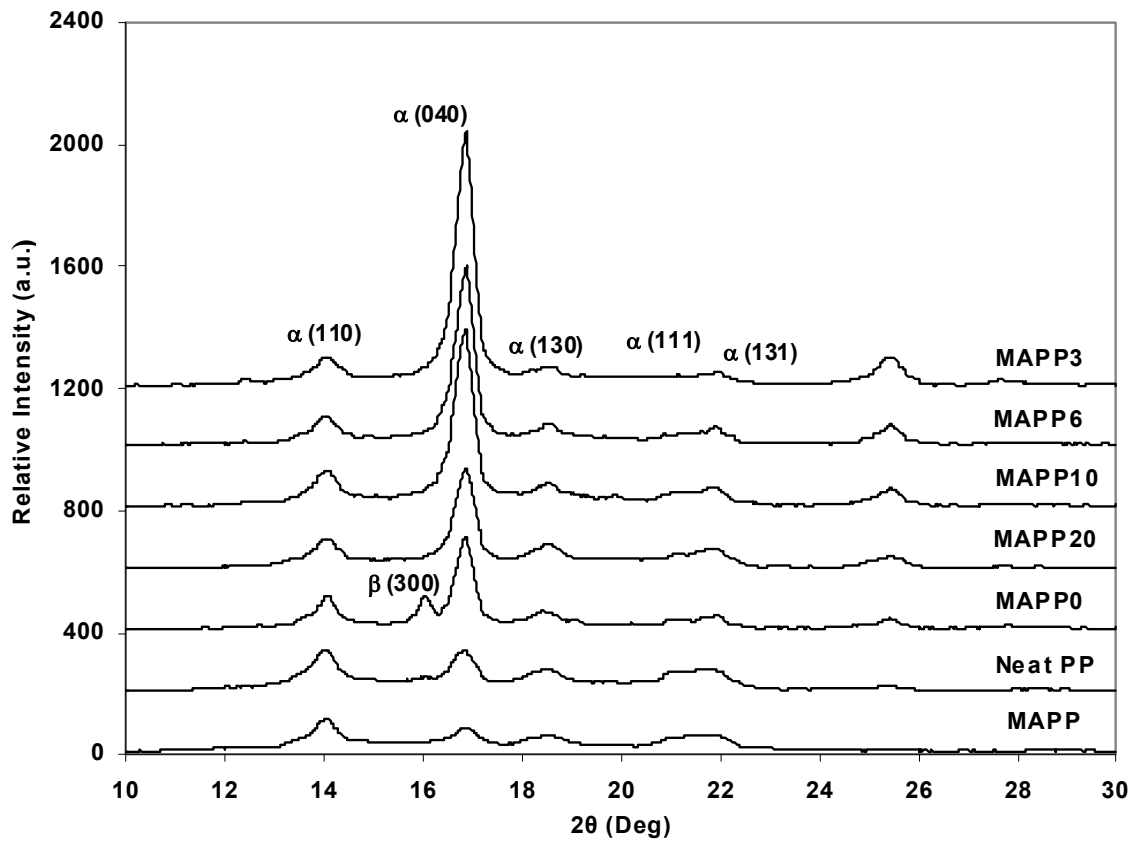


Fig. 3

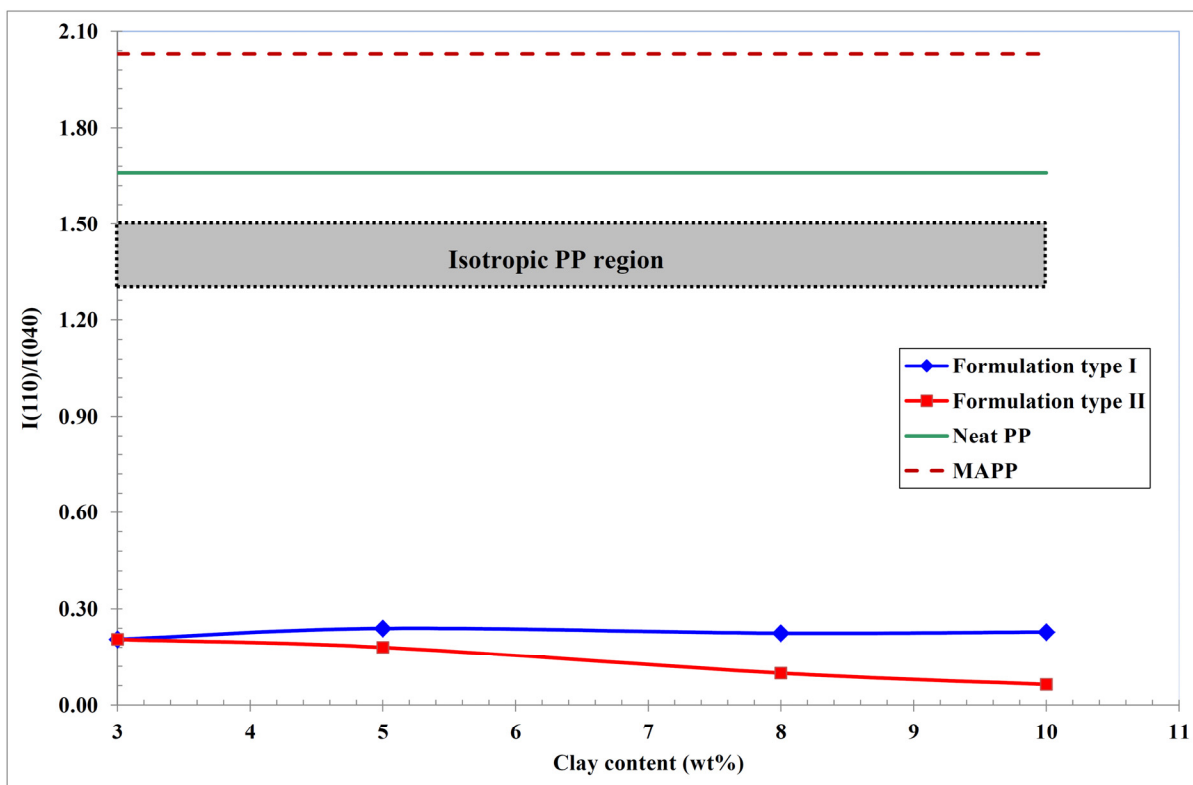


Fig.4

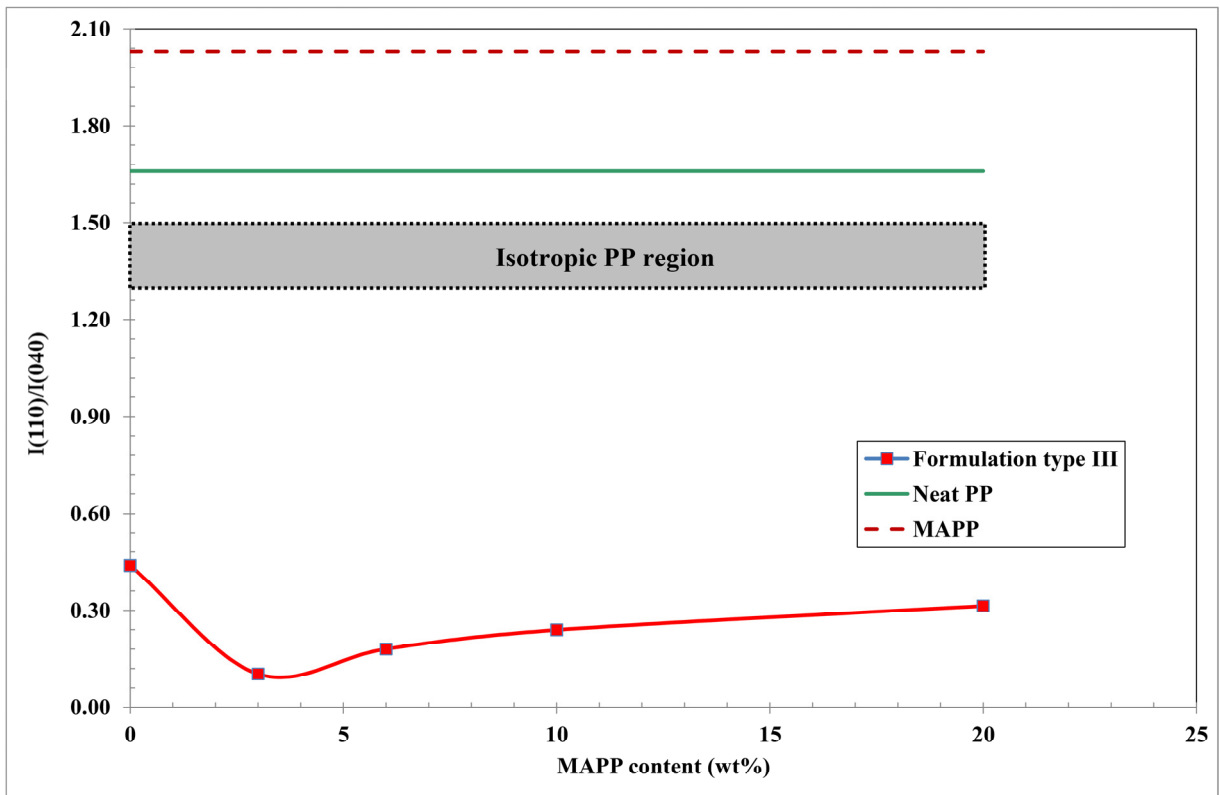


Fig. 5

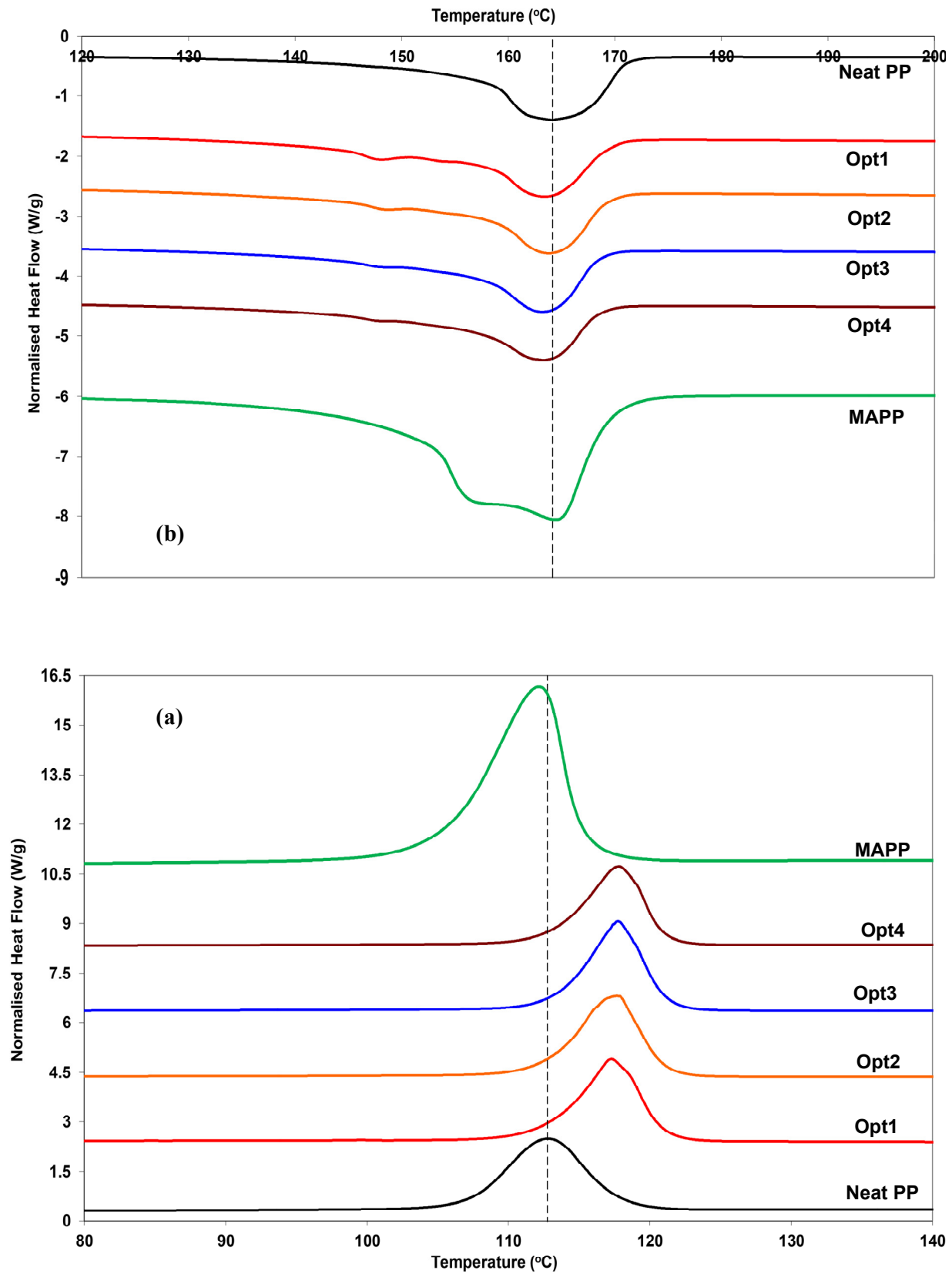


Fig. 6

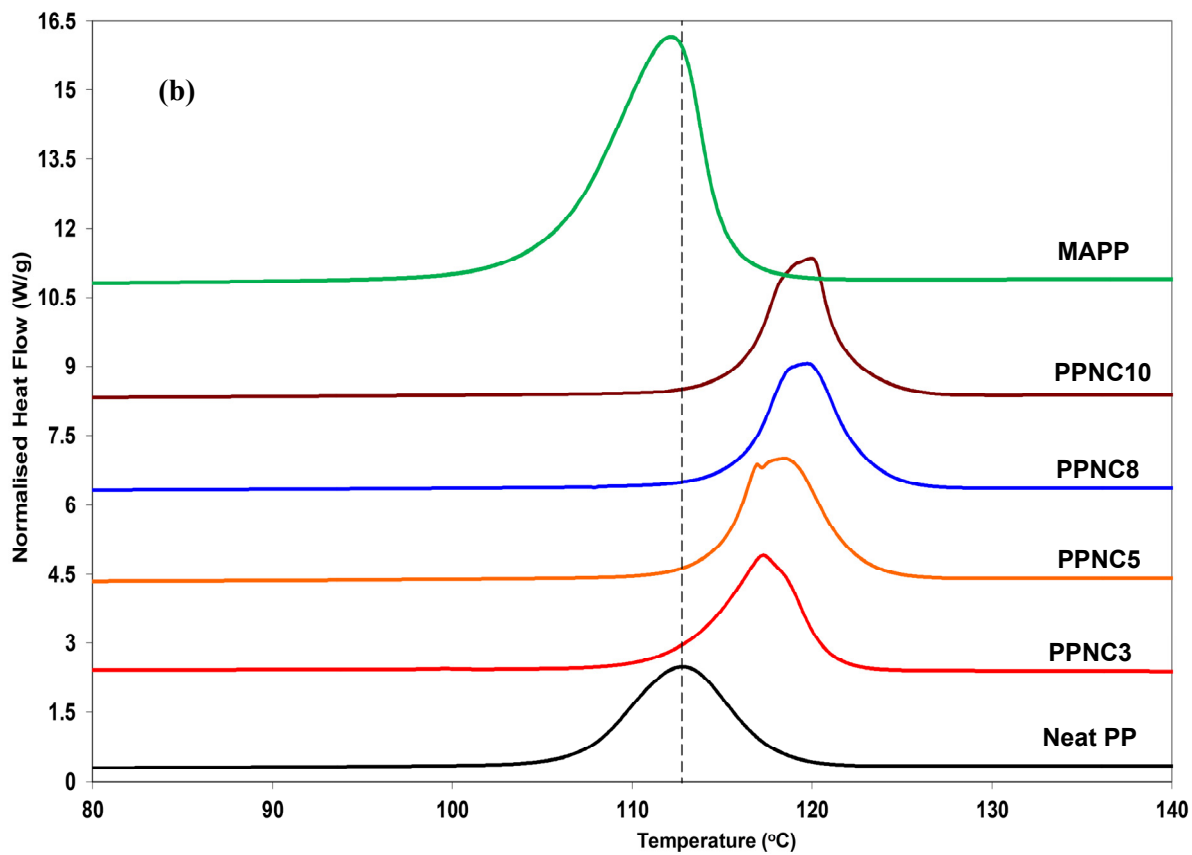
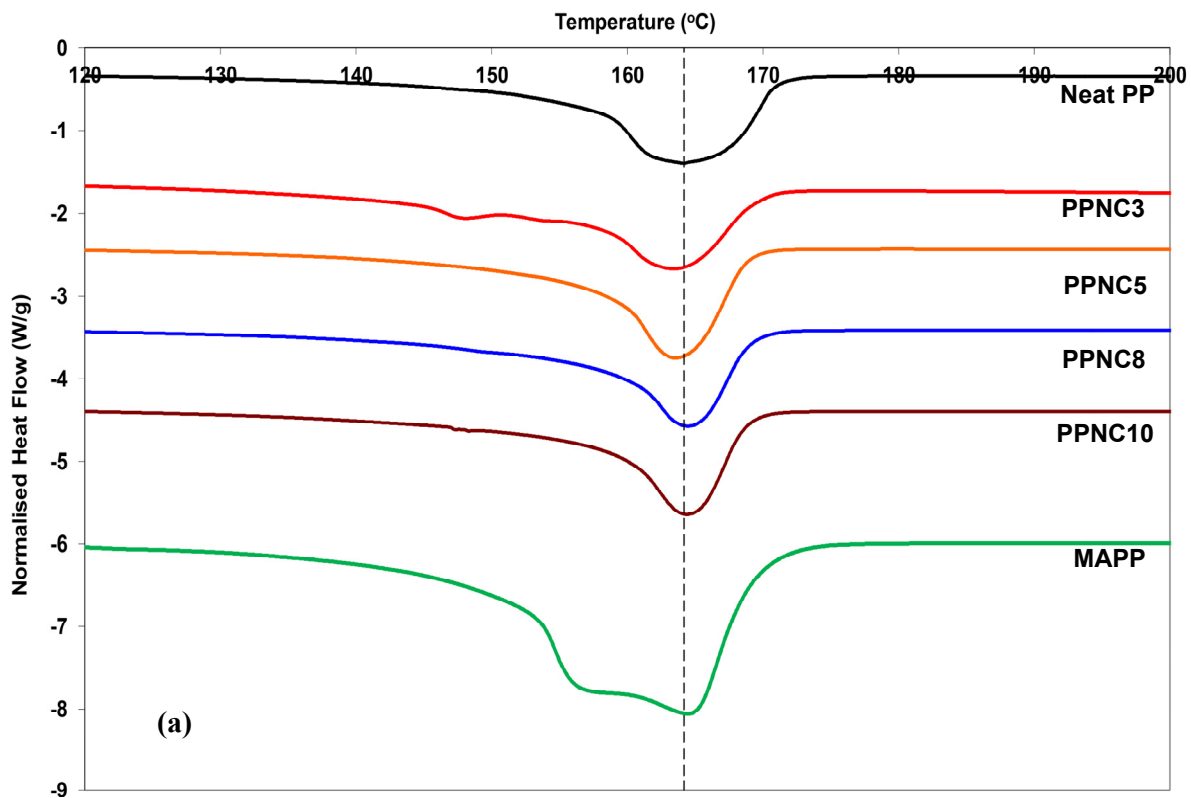


Fig. 7

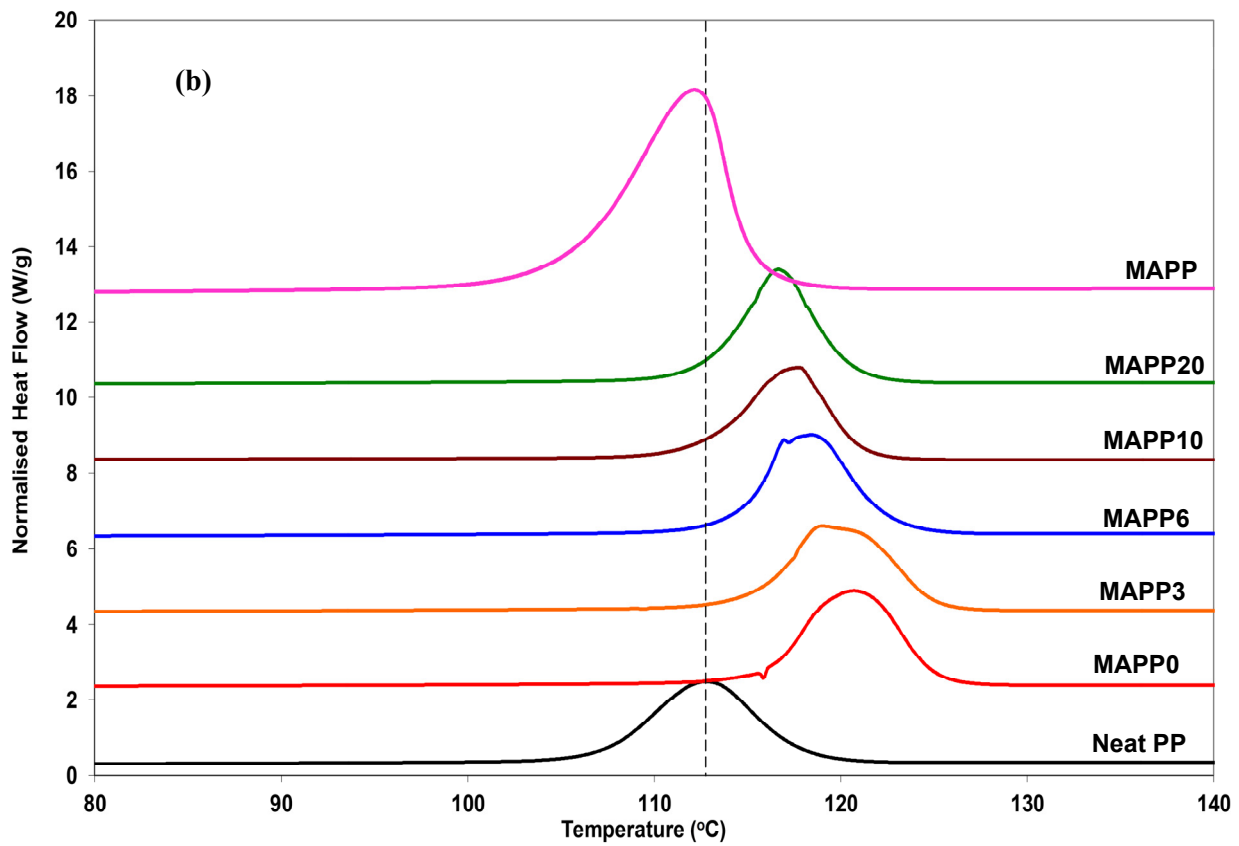
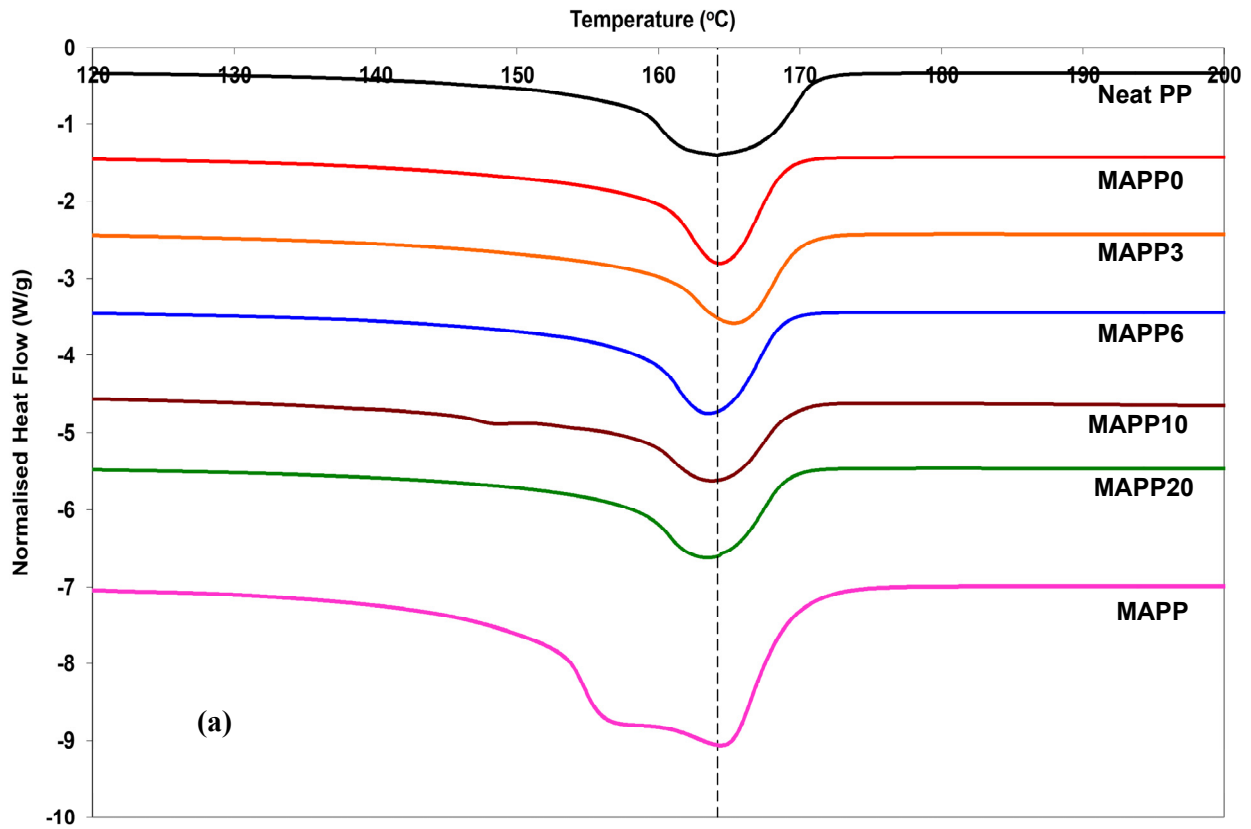


Fig. 8

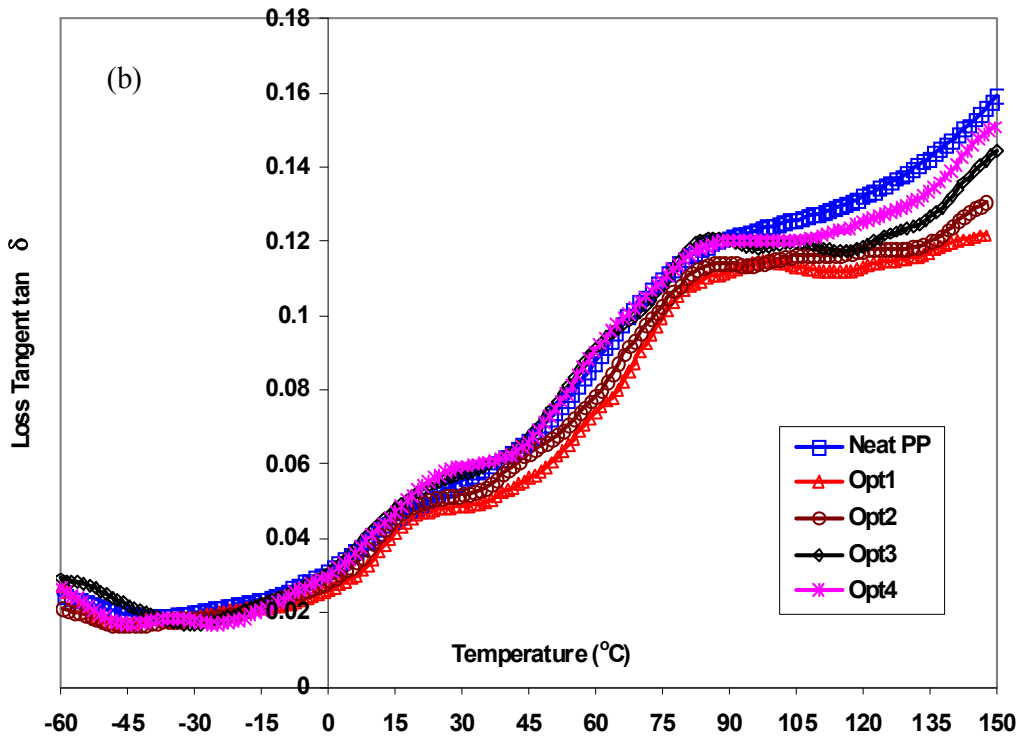
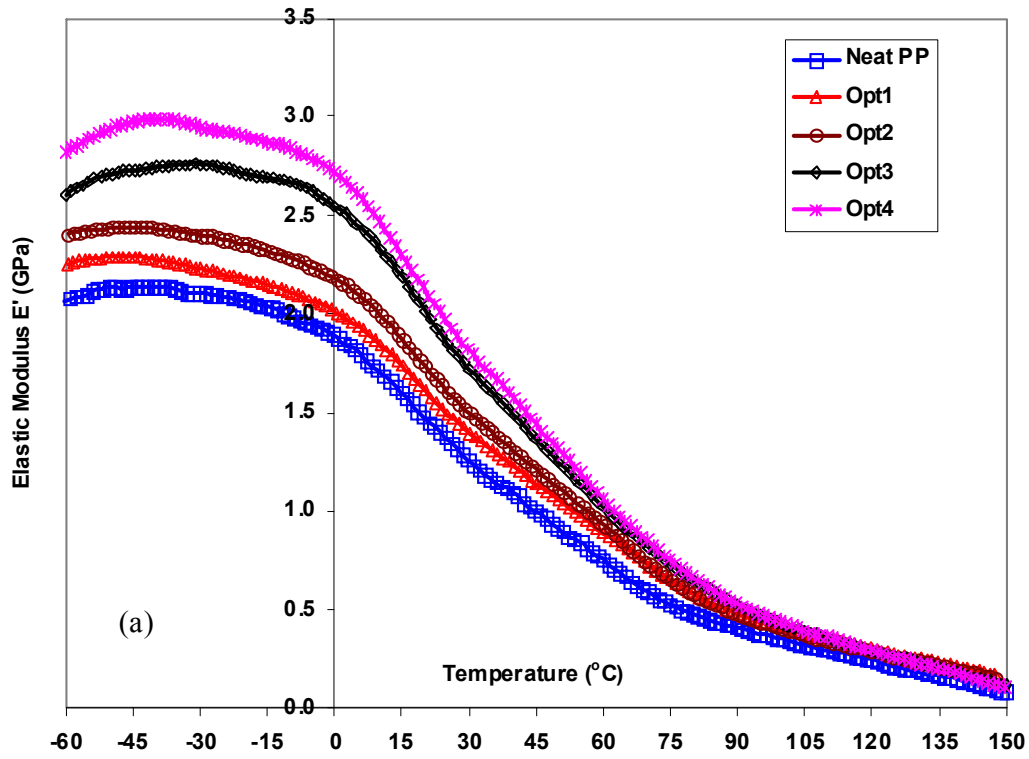


Fig. 9

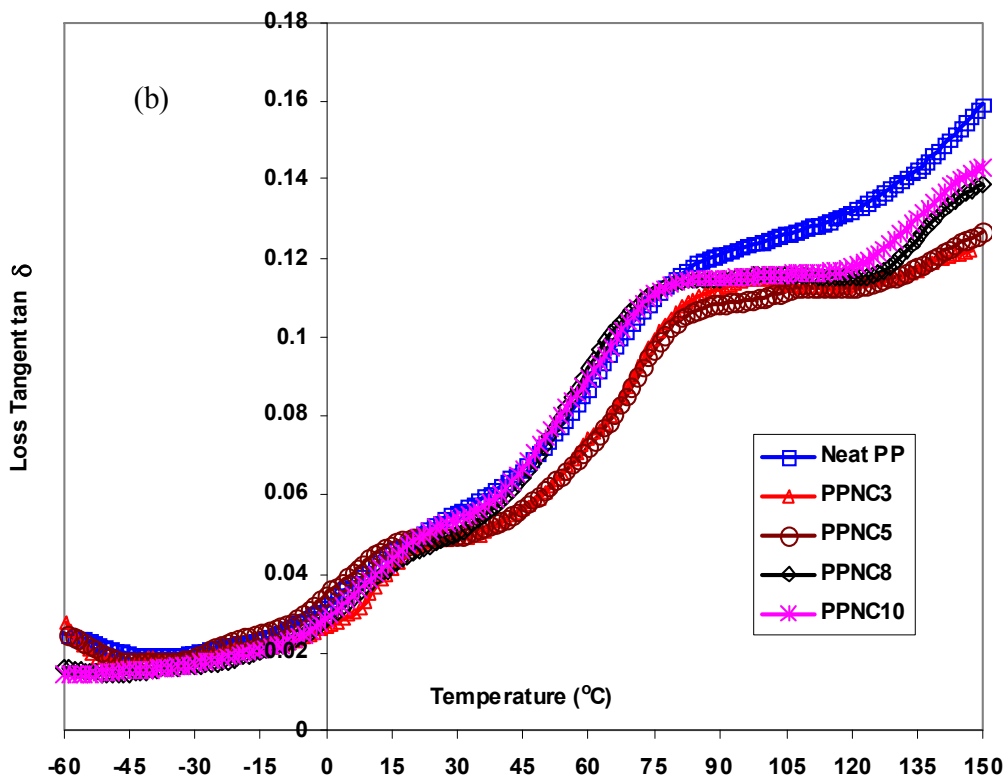
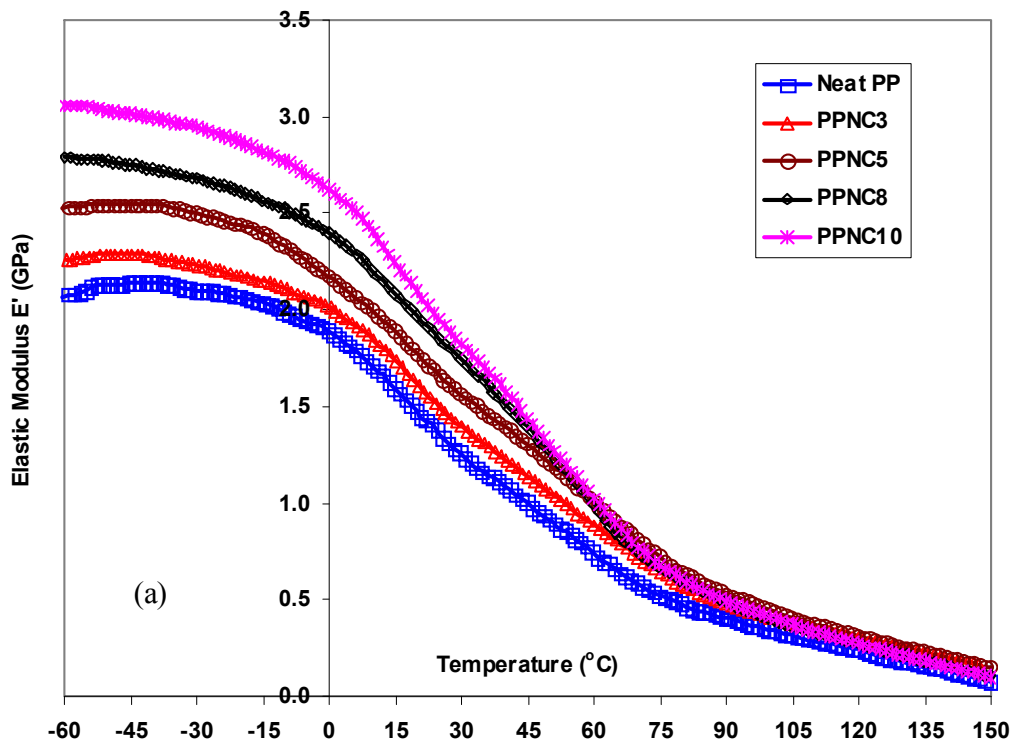


Fig. 10

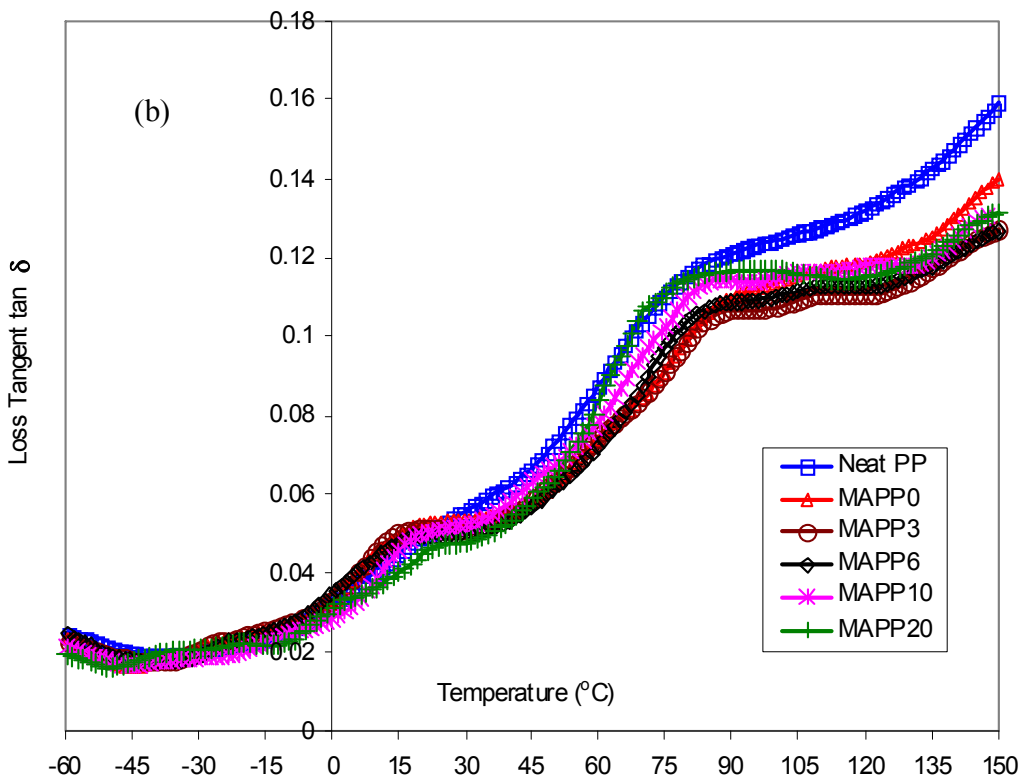
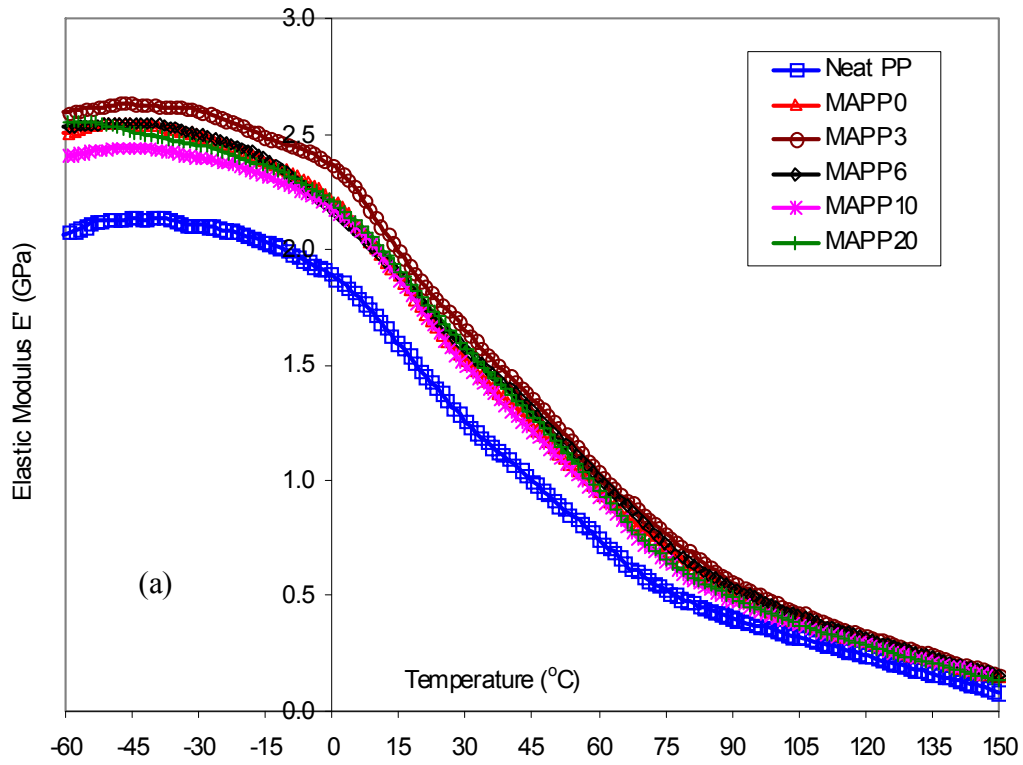


Fig. 11

Table 1 Material formulations of PP/clay nanocomposites

Formulation type	Sample name	Composition (wt%)		
		Clay	MAPP	PP
I	Opt1	3	6	91
	Opt2	5	10	85
	Opt3	8	16	76
	Opt4	10	20	70
II	PPNC3 (Opt1)	3	6	91
	PPNC5	5	6	89
	PPNC8	8	6	86
	PPNC10	10	6	84
III	MAPP0	5	0	95
	MAPP3	5	3	92
	MAPP6 (PPNC5)	5	6	89
	MAPP10 (Opt2)	5	10	85
	MAPP20	5	20	75

Table 2 DSC characteristic parameters and level of crystallinity of PP/clay nanocomposites.

Material type	Clay /MAPP content (wt%)	T_m (°C)	T_c (°C)	ΔH_m (J/g)	X_c (%)
Neat PP	0/0	164.2	112.8	87.32	41.8
MAPP	0/100	164.3	112.0	192.9	92.3
Opt1	3/6	163.3	117.3	92.86	45.8
Opt2	5/10	163.9	117.7	89.06	44.9
Opt3	8/16	163.1	117.8	88.96	46.3
Opt4	10/20	163.3	117.8	82.79	44.0
PPNC3	3/6	163.3	117.3	92.86	45.8
PPNC5	5/6	163.6	118.5	96.32	48.5
PPNC8	8/6	164.4	119.7	89.77	46.7
PPNC10	10/6	164.3	119.9	90.78	48.3
MAPP0	5/0	164.3	120.7	90.08	45.4
MAPP3	5/3	165.3	119.0	86.20	43.4
MAPP6	5/6	163.6	118.5	96.32	48.5
MAPP10	5/10	163.9	117.7	89.06	44.9
MAPP20	5/20	163.5	116.7	91.78	46.2

Table 3 Dynamic elastic moduli E' of PP/clay nanocomposites at various temperatures and related glass transition temperatures (T_g).

	Dynamic elastic modulus* E' (GPa)					T_g (°C)
	-30°C	5°C	25°C	90°C	135°C	
Neat PP	2.10	1.82	1.38	0.41	0.16	14.7
Opt1	2.23 (1.06)	1.93 (1.06)	1.49 (1.08)	0.48 (1.18)	0.23 (1.42)	18.9
Opt2	2.40 (1.14)	2.10 (1.16)	1.60 (1.16)	0.48 (1.18)	0.21 (1.29)	17.7
Opt3	2.76 (1.31)	2.45 (1.35)	1.85 (1.35)	0.52 (1.27)	0.20 (1.23)	18.8
Opt4	2.95 (1.40)	2.61 (1.44)	1.97 (1.43)	0.53 (1.30)	0.20 (1.24)	21.2
PPNC3	2.23 (1.06)	1.93 (1.06)	1.49 (1.08)	0.48 (1.18)	0.23 (1.42)	18.9
PPNC5	2.50 (1.19)	2.09 (1.15)	1.67 (1.21)	0.54 (1.32)	0.23 (1.42)	14.7
PPNC8	2.68 (1.27)	2.31 (1.27)	1.86 (1.35)	0.49 (1.20)	0.19 (1.17)	17.4
PPNC10	2.95 (1.40)	2.53 (1.39)	1.95 (1.42)	0.50 (1.22)	0.19 (1.17)	20.0
MAPP0	2.50 (1.19)	2.13 (1.17)	1.63 (1.19)	0.51 (1.25)	0.22 (1.35)	15.9
MAPP3	2.60 (1.24)	2.28 (1.25)	1.76 (1.28)	0.56 (1.37)	0.24 (1.48)	14.7
MAPP6	2.50 (1.19)	2.09 (1.15)	1.67 (1.21)	0.54 (1.32)	0.23 (1.42)	14.7
MAPP10	2.40 (1.14)	2.10 (1.16)	1.60 (1.16)	0.48 (1.18)	0.21 (1.29)	17.7
MAPP20	2.45 (1.16)	2.12 (1.17)	1.68 (1.22)	0.49 (1.20)	0.21 (1.29)	21.5

* The values in parentheses are the relative dynamic elastic moduli of nanocomposites to those of neat PP.